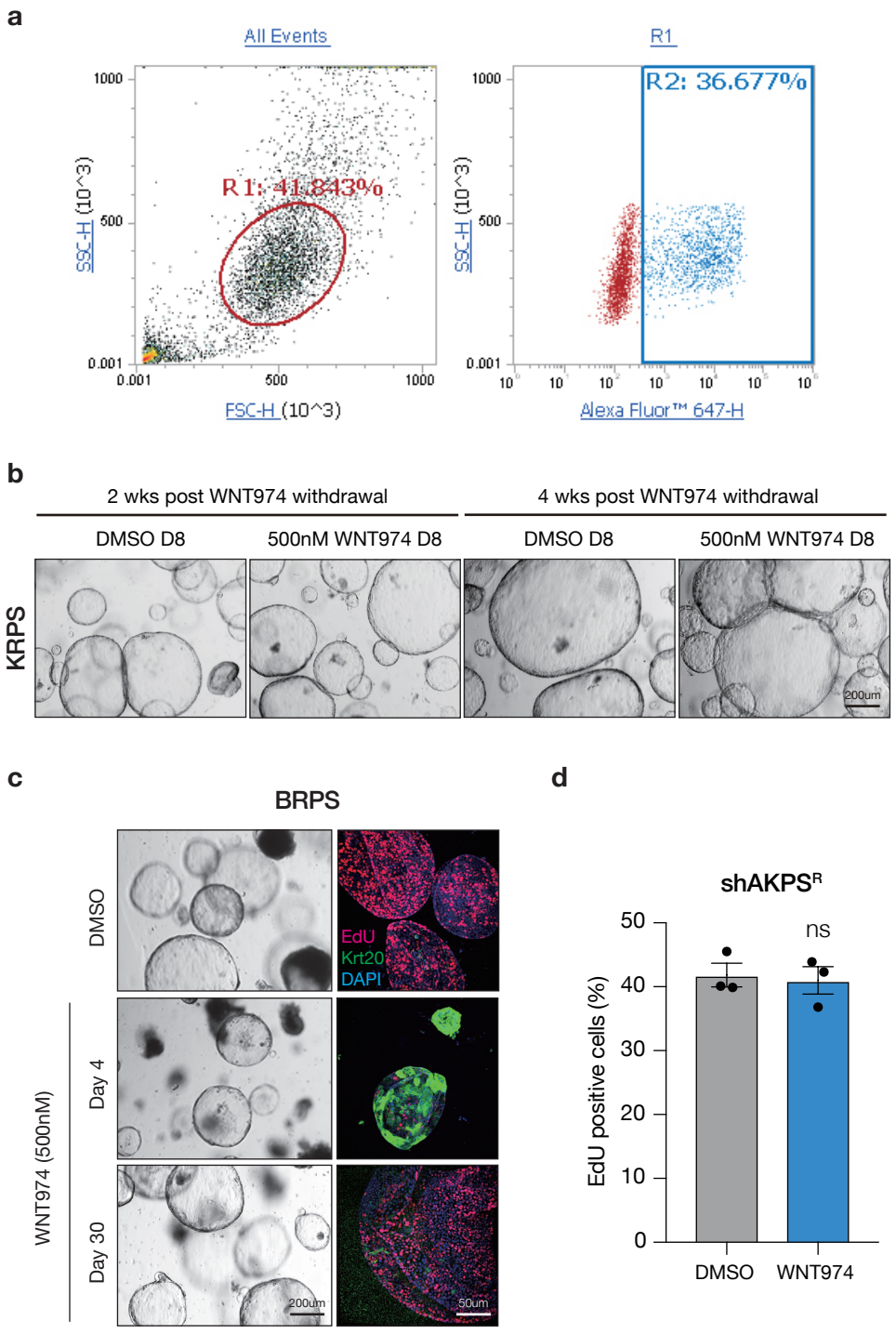

Figure S1. Kras/Braf, p53 and Smad4 mutations enable sustained Wnt independence. **a.** Representative flow cytometry plots showing the gating strategy for EdU flow cytometry. Live cells are gated in R1, EdU positive cells (labeled with Alexa Fluor™ 647) are gated in R2, as a percentage of the live gate. **b**. Bright-field images of WNT974-resistant KRPS cells re-challenged with WNT974 two weeks and four weeks after WNT974 withdrawal. **c**. Bright field and immunofluorescent images of BRPS organoids treated with DMSO or WNT974. **d**. Percentage EdU positive cells measured by flow cytometry of Apc restoration resistant shAKPS organoids treated with DMSO or 500nM WNT974 for 4 days. Error bars show +/- SEM, p-value calculated by two-sided t-test with Welsh's correction.

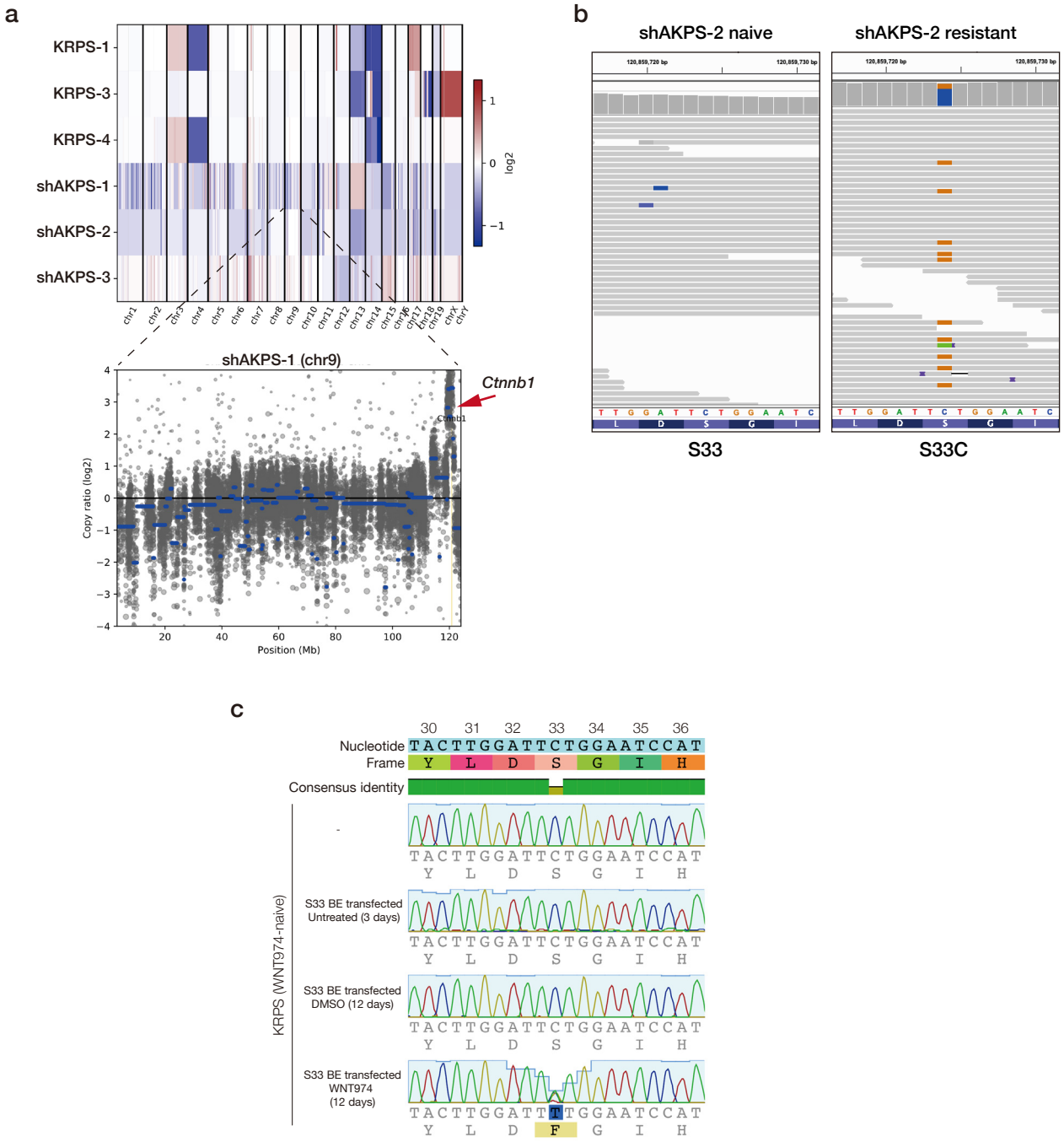

Figure S2. Downstream activation of WNT signaling in two WNT974-resistant organoid lines. a. Copy number alterations in WNT974-resistant KRPS lines and Apc restoration-resistant shAKPS lines (upper), Ctnnb1 amplification in shAKPS-1 is highlighted (lower). **b**. IGV plot showing the emergence of a Ctnnb1 hotspot mutation in resistant shAKPS2 population. **c**. WNT974-naive KRPS organoids carrying base-edited induced Serine 33 mutations are enriched when cultured in the presence of 500nM WNT974, but not in DMSO.

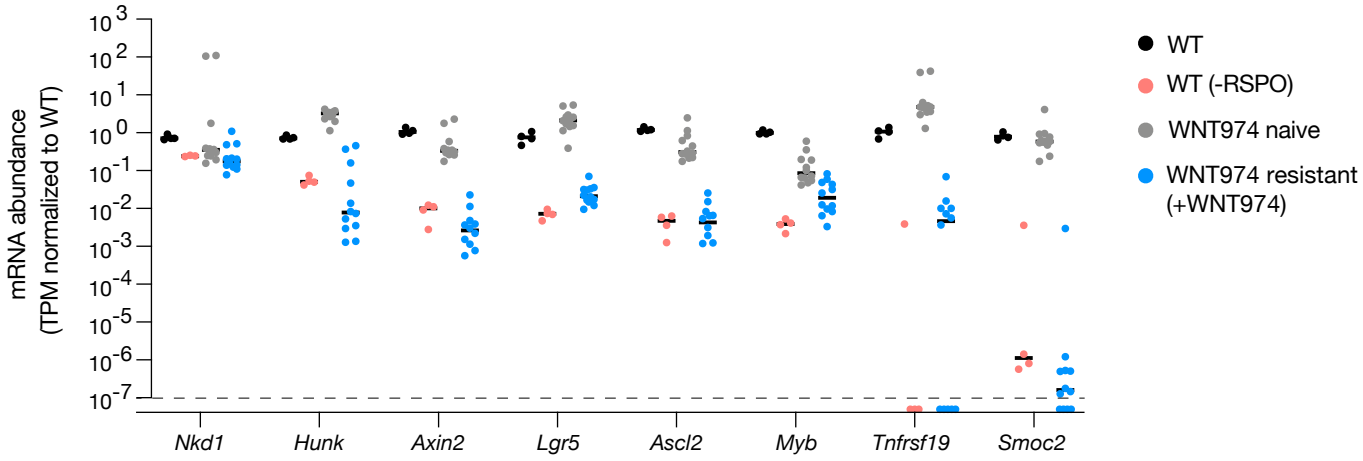

Figure S3. Expression of WNT target genes in WT, drug-naive, and drug-resistant KRPS/BRPS/shAKPS organoids. a. Dot plot showing normalized transcripts per million (TPM) from RNAseq of: WT organoids in the presence (black circles) or absence (red circles) or RSPO1 for 3 days, and KRPS/BRPS/shAKPS organoids untreated (grey circles) or treated (blue circles) with WNT974 (500nM). Circles lying along the x-axis showed zero reads in RNAseq and could not be plotted on Log_{10} scale.

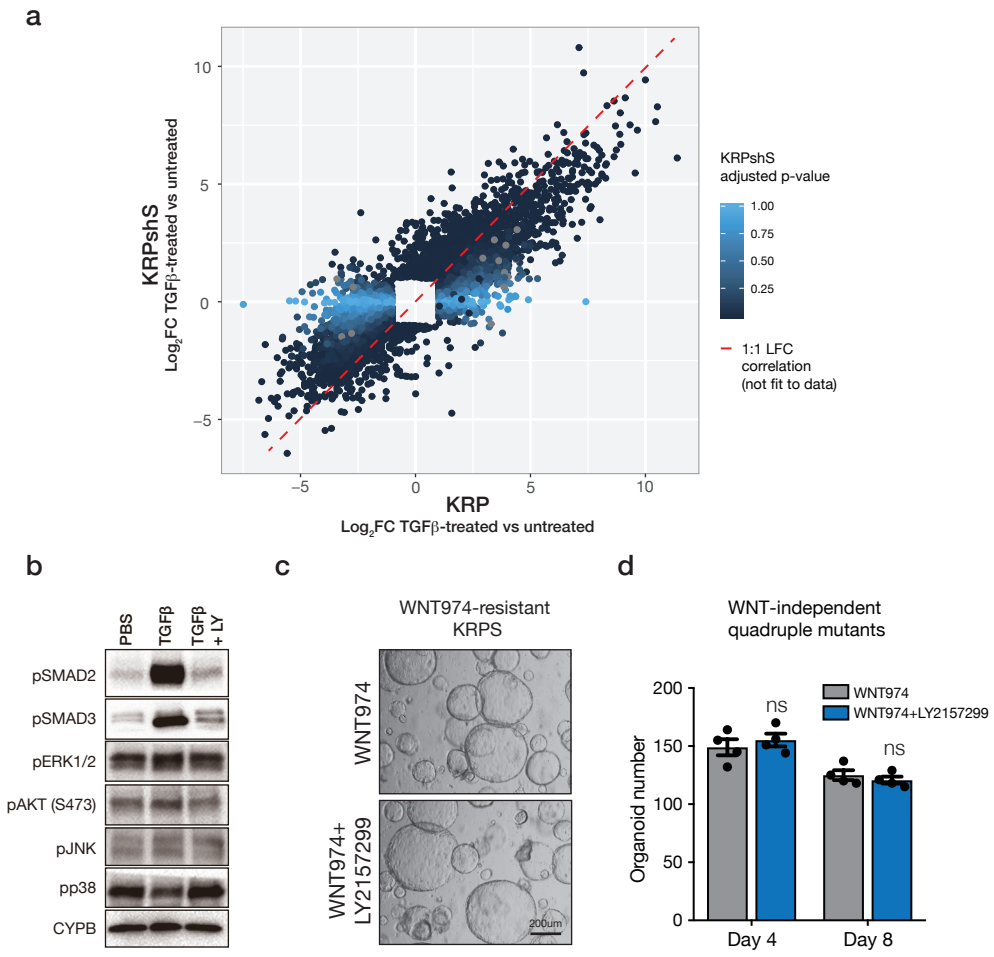

Figure S4. TGFβ induces signaling in the absence of SMAD4 and is not required for the maintenance of WNT independence. a. Scatter plot showing Log2 fold change (Log_2FC) of genes significantly up or downregulated (Log_2FC >1 of <-1 for each condition, padj < 0.01 in KRP) following 3 days of TGFβ treatment (5ng/ml) in either KRP or KRPshS organoids. Color indicates the adjusted p-value for each given gene in KRPshS cells. Gene expression changes in KRP and KRPshS cells are largely similar, despite the depletion of Smad4 protein. **b.** Western blot of KRPshS organoids treated with PBS, TGFβ, or TGFβ/LY2157299 for 24 hours. **c**. Bright field images of WNT974-resistant KRPS organoids treated with 500nM WNT974 or 500nM WNT974 plus 10uM LY2157299 for 8 days. **d.** Quantification of WNT974-resistant KRPS organoids treated with 500nM WNT974 or 500nM WNT974 plus 10uM LY2157299 for 4 days and 8 days (n=4, error bars=SEM, *, $p<0.05$, two-way ANOVA, with Tukey's correction).

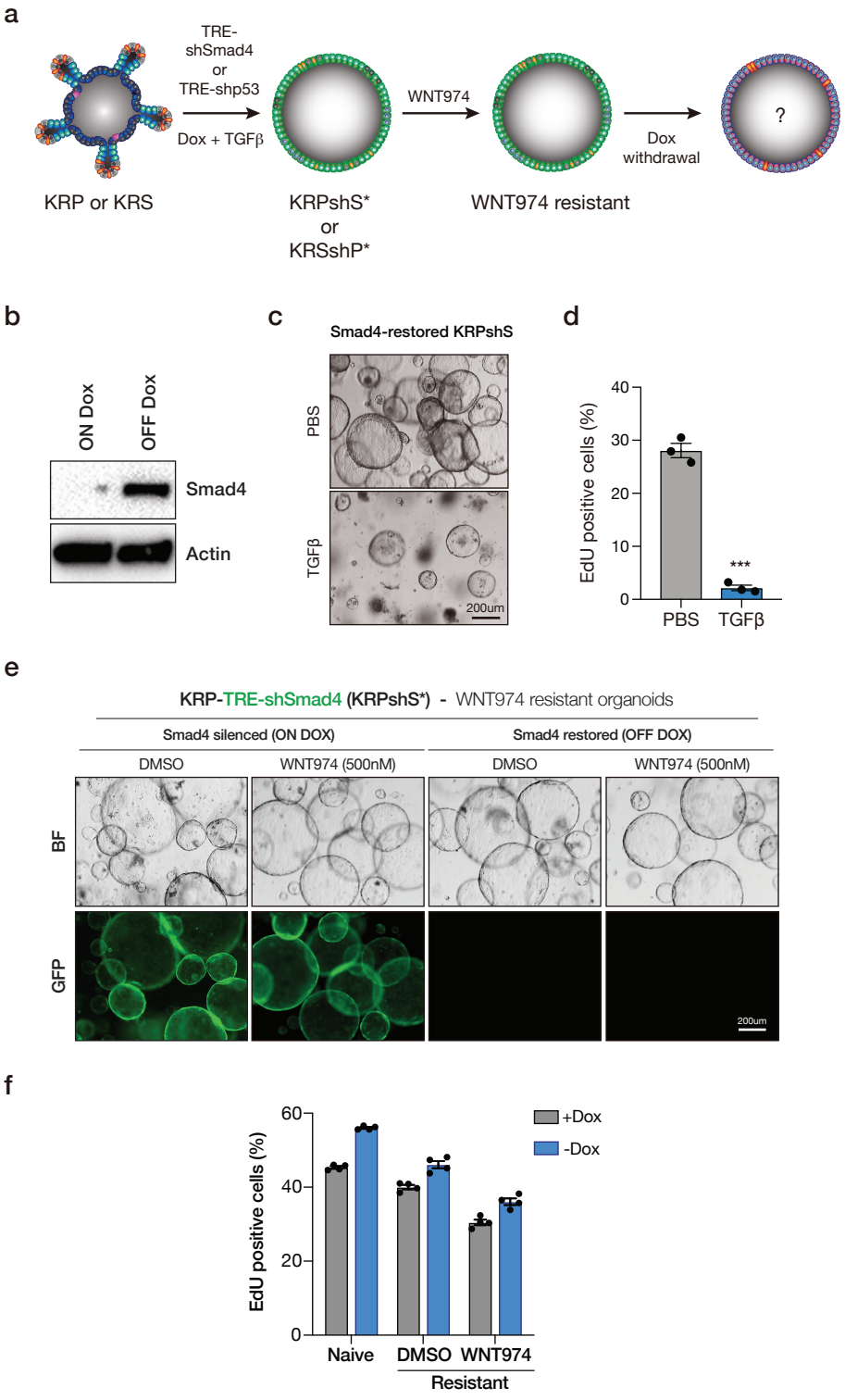

Figure S5. Smad4 loss is not required for the maintenance of WNT independence. a. Schematic diagram of testing the requirement of Smad4 loss and p53 loss in WNT-independent cells using inducible shSmad4 and shp53. **b.** Western blot showing Smad4 restoration in WNT974-resistant KRPshS* withdrawn from Dox for 4 days. **c.** Bright field images of Smad4-restored WNT-independent KRPshS* treated with PBS or TGFβ for 4 days. **d.** EdU flow cytometry of Smad4-restored WNT-independent KRPshS* treated with PBS or TGFβ for 4 days (n=3, error bars=SEM, p-values calculated using a two-sided t-test, with Welsh's correction, ***p<0.001). **e.** Bright field and fluorescent images of Smad4 restoration in KRPshS* WNT974-resistant cells. **f.** Percentage of EdU positive cells in Smad4 restored WNT974-naive KRPshS* and WNT974-resistant KRPshS* lines (n=4, error bars=SEM).

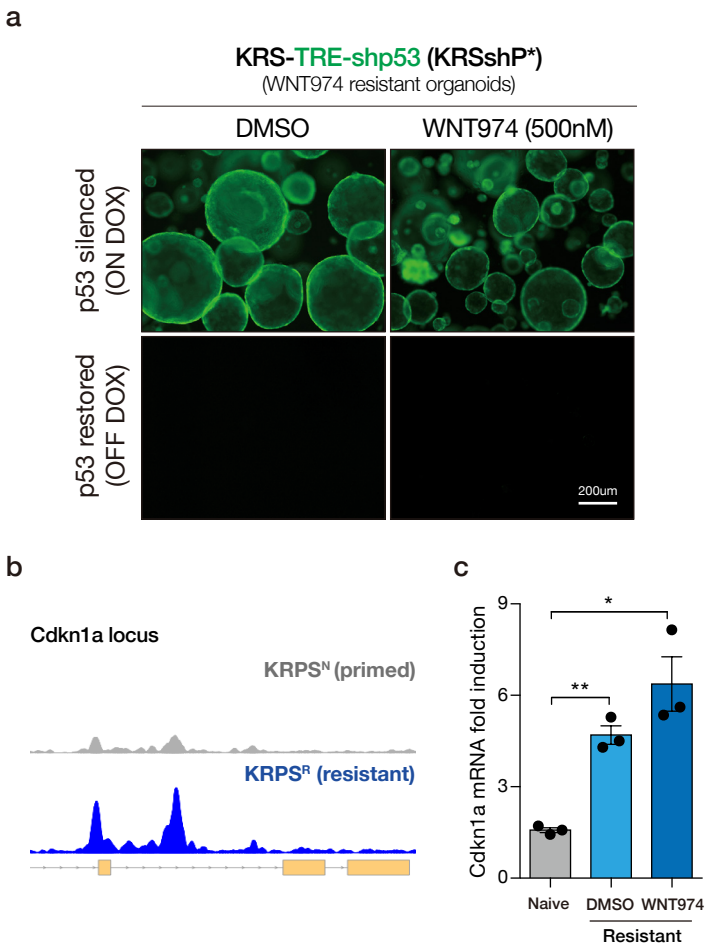

Figure S6. p53 loss is required for the maintenance of WNT independence. a. GFP fluoresent images of KRSshP* WNT974-resistant cells cultured +/- Dox in DMSO or WNT974 (500nM), as indicated. GFP is linked to shRNA transcription downstream of the TRE promoter. These images show effective shRNA silencing after Dox withdrawal. **b.** Chromatin accessibility (measured by ATACseq) at the Cdkn1a locus in WNT974-resistant KRPS organoids, compared to WNT974-naive KRPS cells. **c.** qRT-PCR analysis of Cdkn1a in WNT974-naive and WNT974-resistant KRSshP* cells after p53 restoration. Cdkn1a mRNA fold induction is calculated relative to mRNA abundance in isogenic cells on Dox (n=3, error bars=SEM, p-values calculated using a two-sided t-test, with Welsh's correction, *, $p<0.05$).

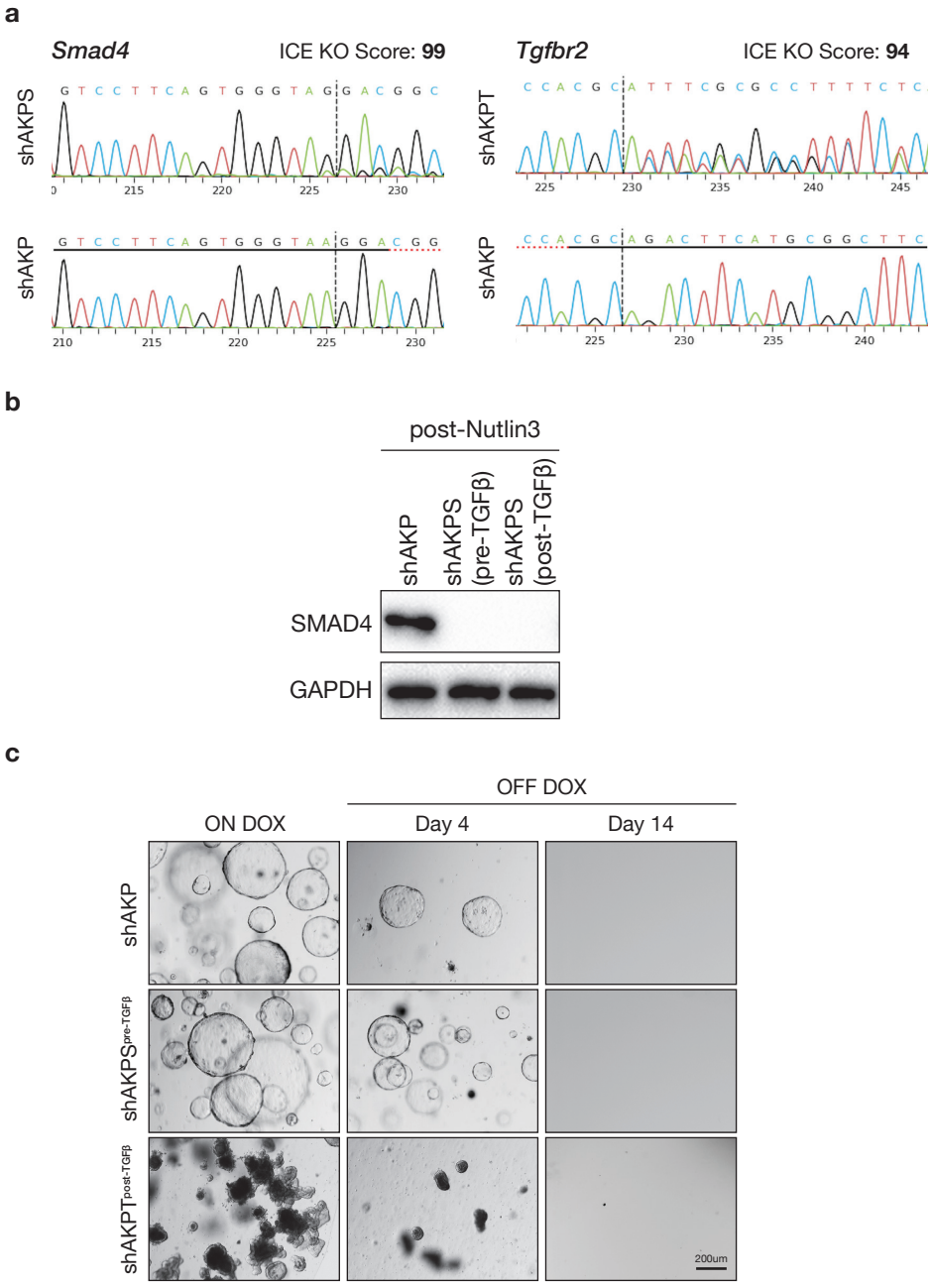

Figure S7. Validation of TGFβ-naive shAKPS cells for transplantation. a. Synthego ICE sequence analysis of Nutlin3-selected, TGFβ-naive shAKPS and TGFβ-treated shAKPT organoids before transplantation. sgRNA targeting sequence is highlighted by black solid line, PAM sequence is highlighted by red dash line, Cas9 cleavage site is labeled by vertical black dash line. **b.**Western blot shows depletion of SMAD4 in both pre- and post-TGFβ organoids. **c.** Bright field images of shAKP, shAKPS (pre-TGFβ) and shAKPT (post-TGFβ) demonstrating that they were unable to escape Apc restoration prior to *in vivo* transplantation.

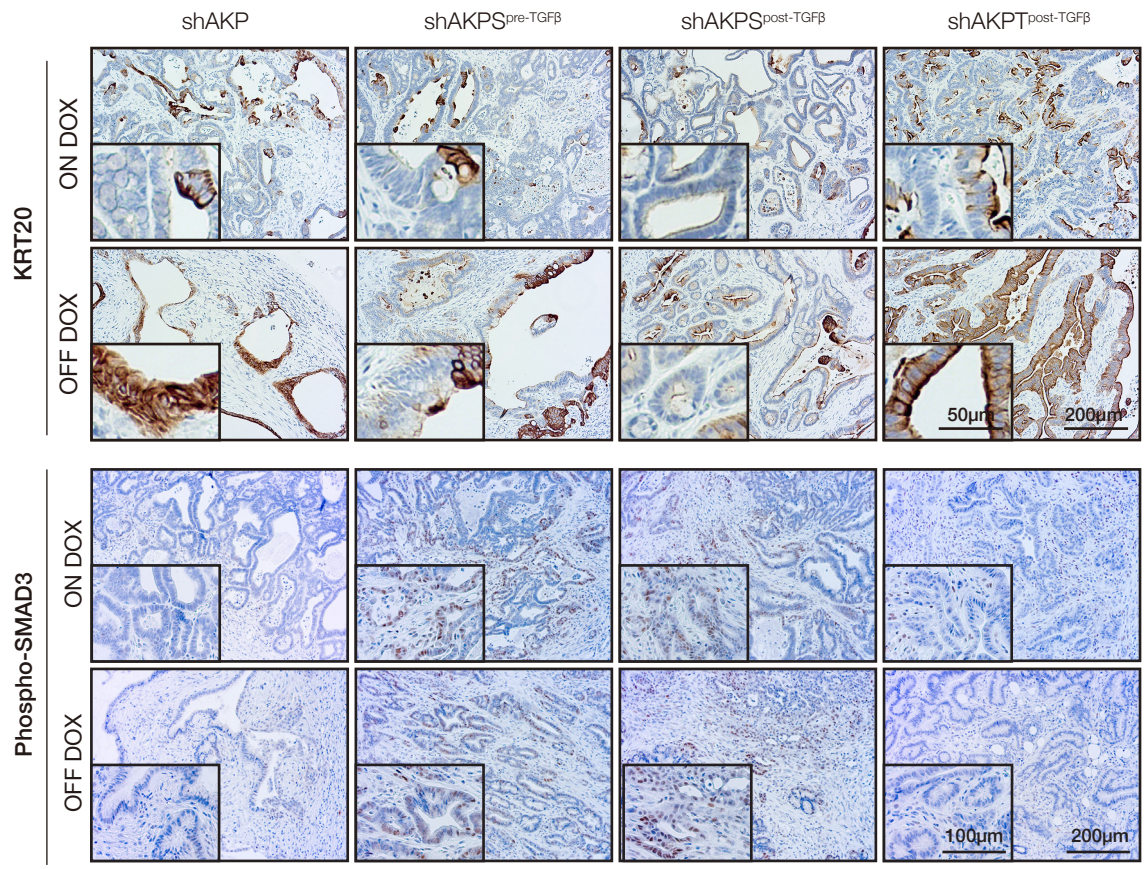

Figure S8. TGFβ in the tumor microenvironment drives WNT independence. ***Upper panels*****:** Keratin20 (KRT20) staining on tumor sections from Dox-treated (Apc silenced) and Dox-withdrawn (Apc restored) mice. Both shAKP and shAKPT show widespread differentiation following Apc restoration. Differentiation is not elevated in post-TGFβ-treated shAKPS after Apc restoration. A mixed response is observed in pre-TGFβ-treated shAKPS after Apc restoration**.** ***Lower panels:*** Phospho-SMAD3 staining on tumor sections as above. shAKPS transplants show strong phospho-SMAD3 stainings in the epithelial cells, however, shAKP and shAKPT show weak or no phospho-SMAD3 staining in epithelial cells.

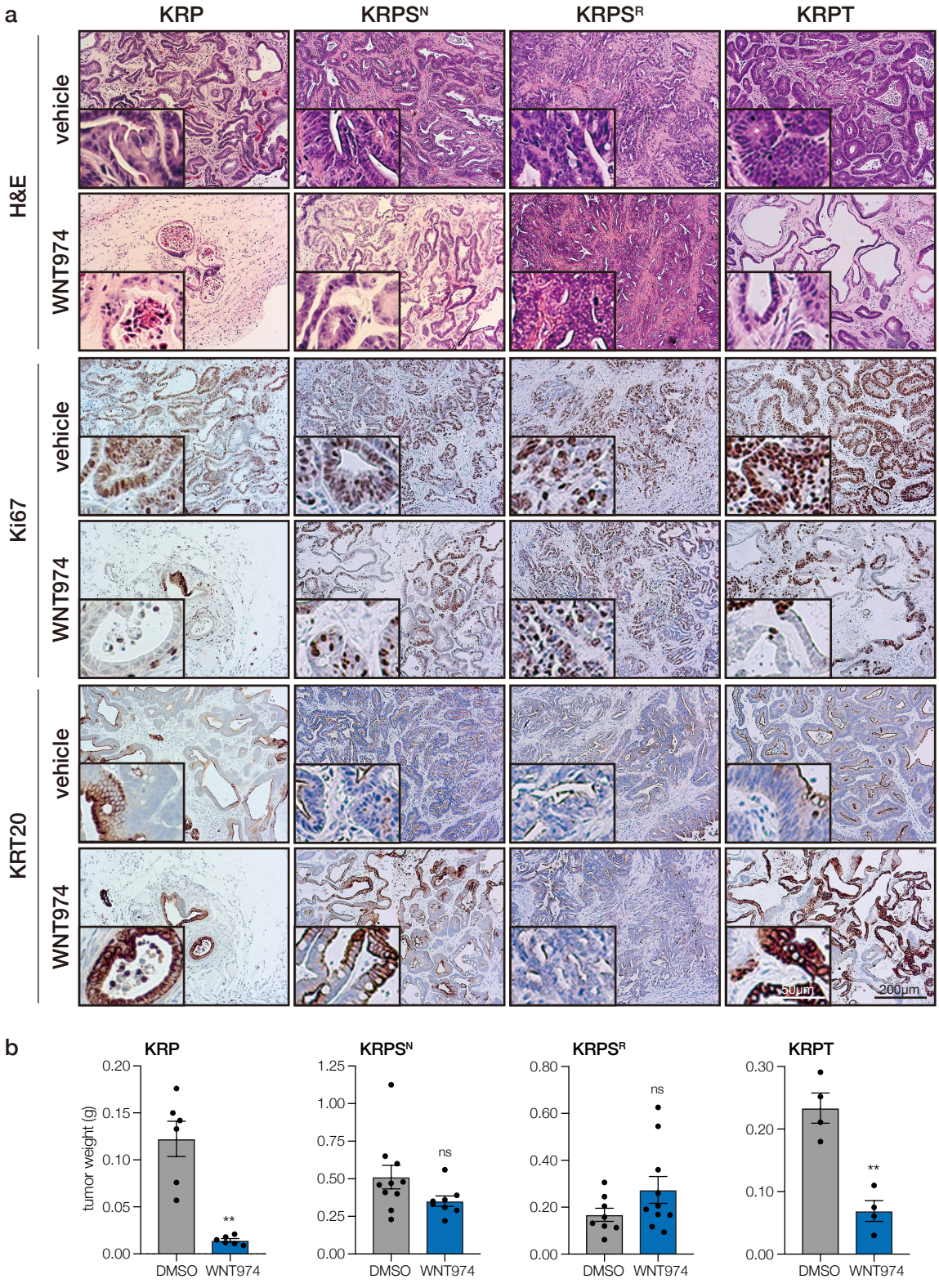

Figure S9. In vivo WNT974 treatment response mirrors in vitro response. **a**. Immunohistochemical stains of organoid transplants treated with vehicle or WNT974 for 2 weeks. **b.** Quantification of tumors weight. NOTE: y-axis scale is different for each genotype to ensure the distribution of values is clearly visible. Error bars represent +/- SEM, n≥4, **p<0.01, calculated by two-sided t-test, with Welsh's correction.

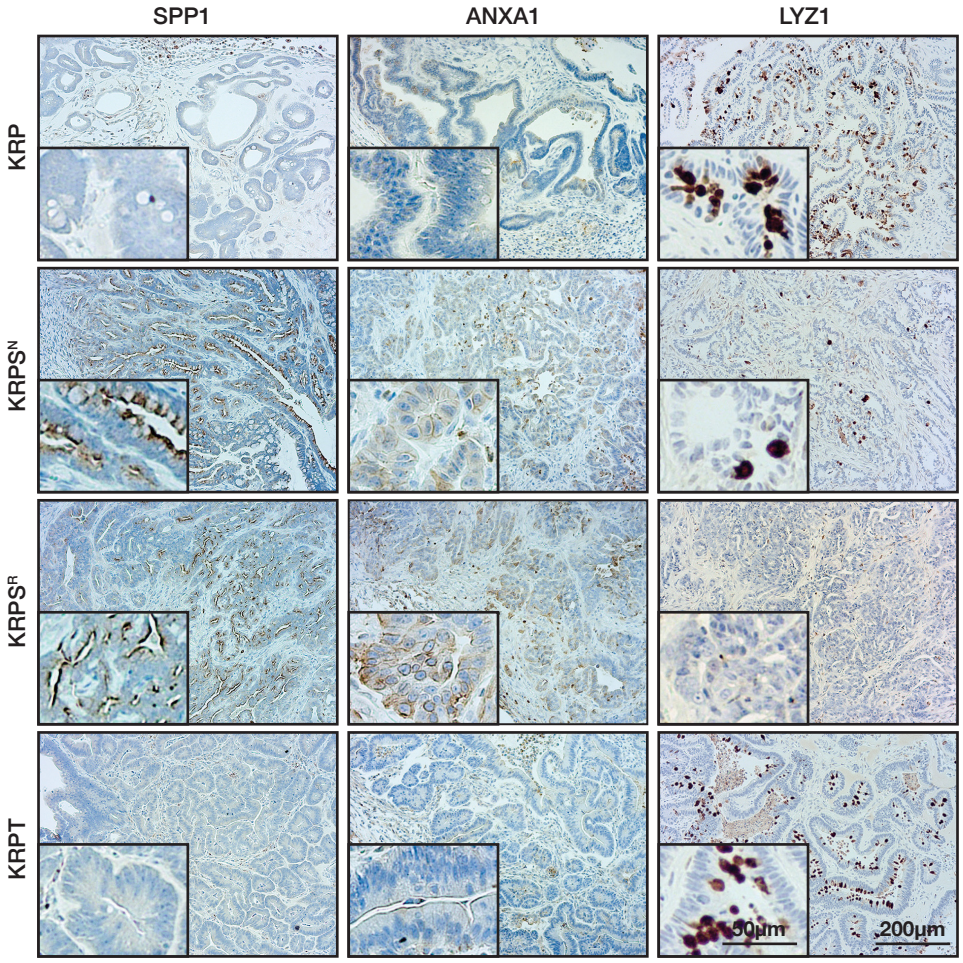

Figure S10. WNT-independent KRPS organoids show fetal-like characteristics *in vivo*. Immunohistochemical stains for Osteopontin (SPP1), Annexin A1 (ANXA1) and Lysozyme (LYZ1) in organoid-derived tumors, as labeled. TGFβ-primed ($KRPS^N$) and WNT974-resistant ($KRPS^R$) tumors, but not WNT-dependent KRP and KRPT tumors, show elevated SPP1, ANXA1 stainings and reduced LYZ1-positive Paneth cells.

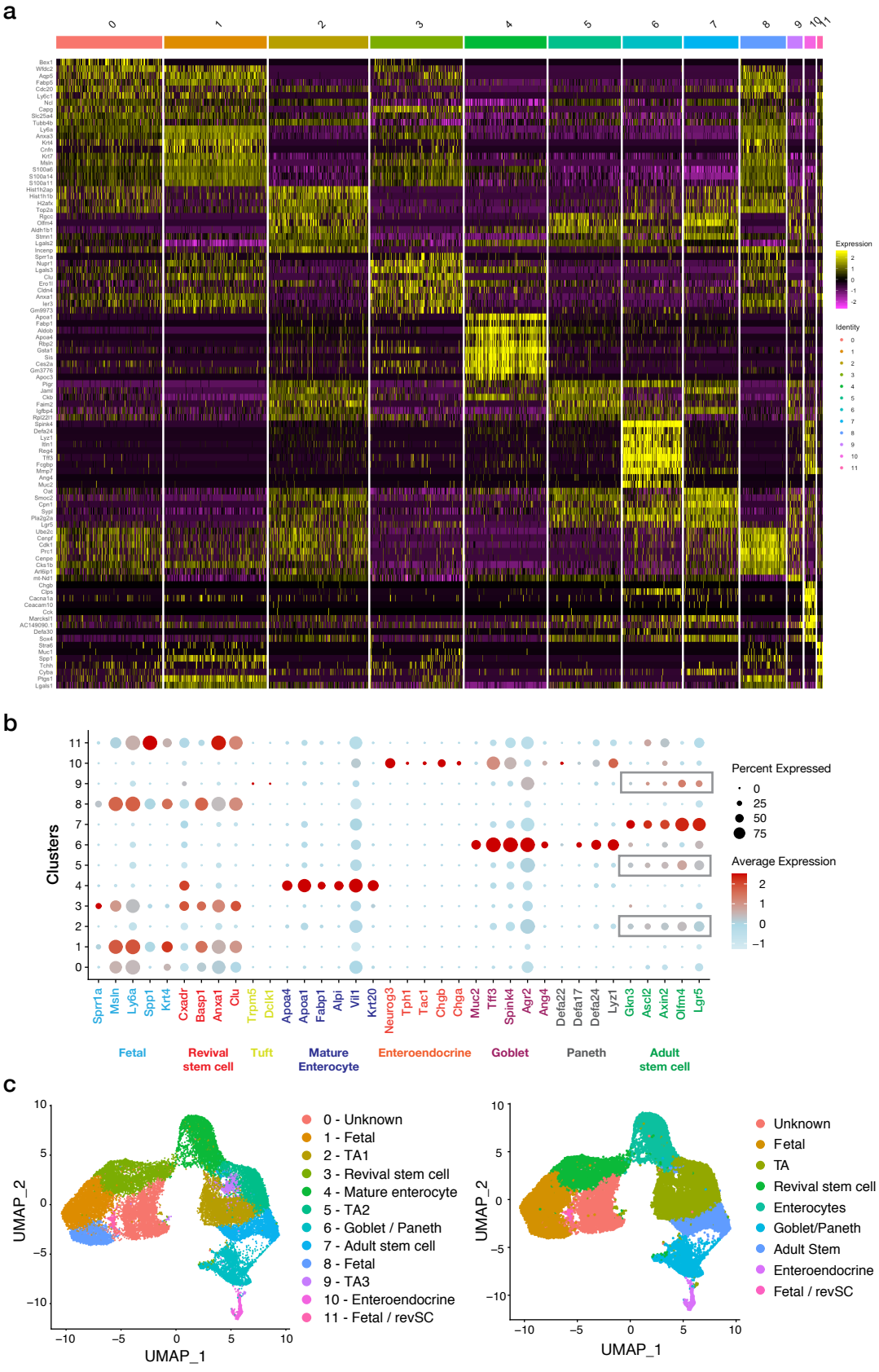

Figure S11. Characterization of clusters and identification of cell-types in organoids. a. Heatmap showing top 10 most differentially expressed genes in each scRNAseq cluster. **b.** Dotplot showing expression of known cell-type specific markers. Size indicates the number of cells within the cluster that show expression of that gene, color reflects mean expression within the cluster. Clusters 2, 5, and 9 did not have a clear pattern of expression associated with cell types shown here, but did have moderate expression of adult stem cell markers (grey boxes). We termed these clusters as transmit amplifing cells: TA1, TA2, TA3. Clusters 0 showed weak expression of cell type markers. We labeled this cluster "Unknown". **c.** Clusters were reclassified based on marker expression above, and TA and Fetal clusters were merged for clarity.

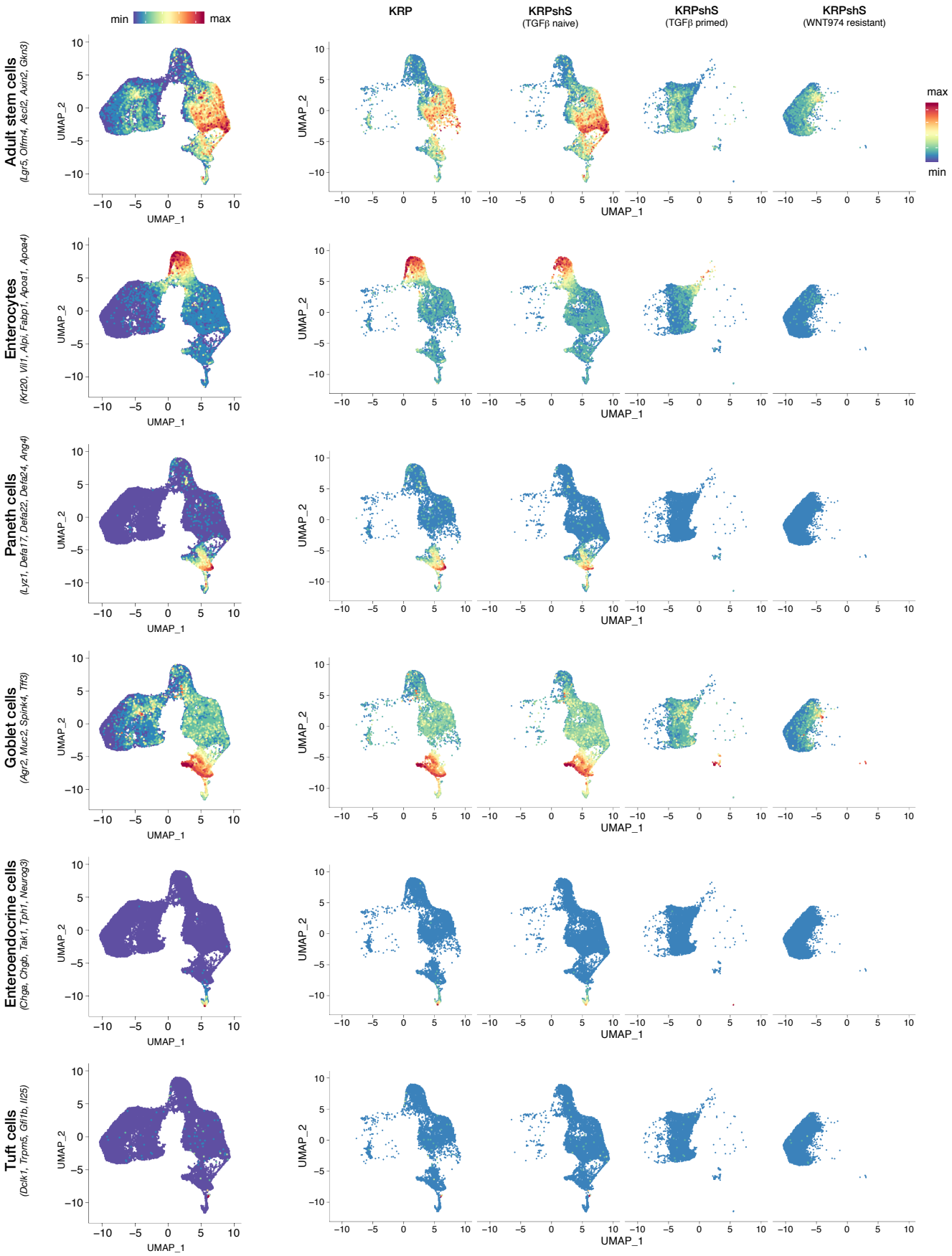

Figure S12. Cluster identity by marker gene expression. Merged (left) and individual UMAP plots showing relative mean expression of marker genes (as labeled). Secretory lineages (goblet and Paneth cells, but not enteroendocrine cells) were grouped as one cluster in our analysis. Tuft cells were not identified as an separate cluster in our analysis, likely owing to the very small number of positive cells.

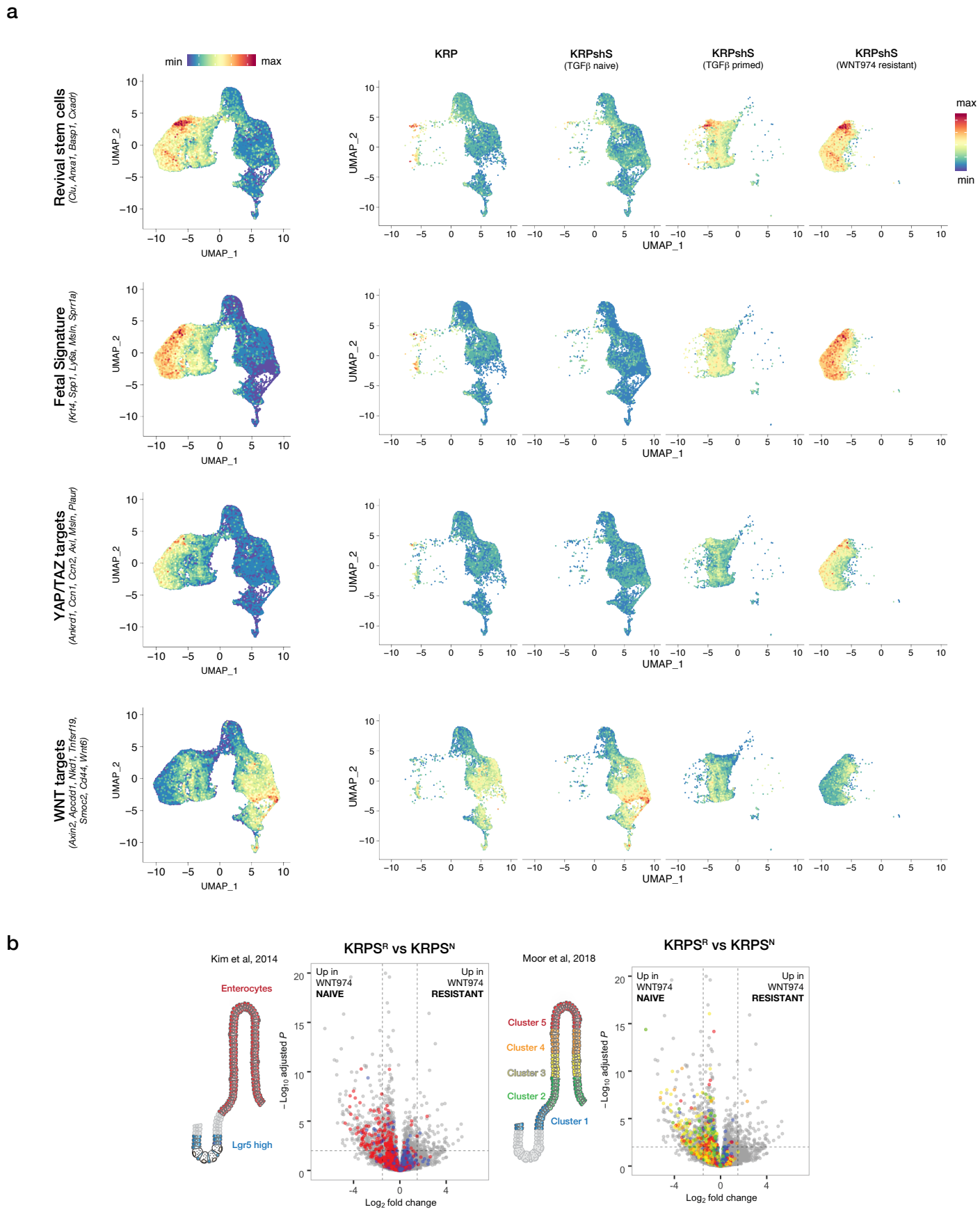

Figure S13. Cluster identity by marker gene expression. a. Merged (left) and individual UMAP plots showing relative mean expression of marker genes (as labeled). **b**. Volcano plots of bulk RNAseq of isogenic WNT974-naive ($KRPS^N$) and WNT974-resistant ($KRPS^R$) organoids (all TGFβ-treated), showing reduced expression of enterocyte markers in WNT974-independent organoids.

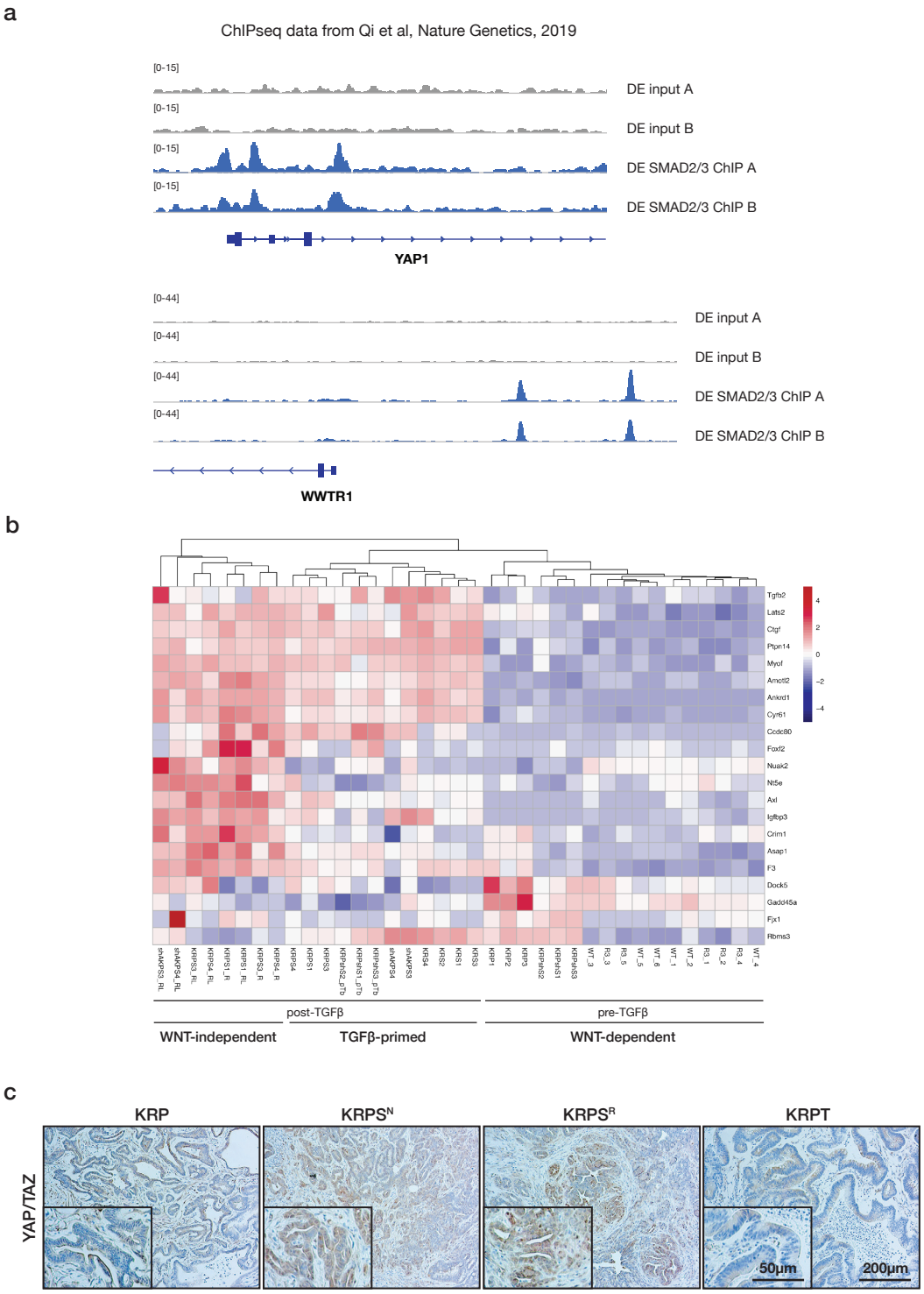

Figure S14. YAP/TAZ transcriptional signature defines TGFβ-primed and WNT independent organoids. **a.** Peak plots of published ChIPseq SMAD2/3 binding on promoter and enhancer regions of *YAP1* and *WWTR1 (TAZ)* in definitive endoderm (DE) derived by *in vitro* hESC differentiation (Qi et al, Nat Gen, 2019). **b.** Unsupervised clustering of organoid RNAseq on YAP/TAZ targets separates all the genotypes into pre-TGFβ, post-TGFβ, and WNT-independent subtypes. **c.** Tumor sections from indicated genotypes stained for YAP/TAZ reveal increased and nuclear localization of YAP/TAZ in TGFβ-primed ($KRPS^N$) and WNT-independent tumors ($KRPS^R$).

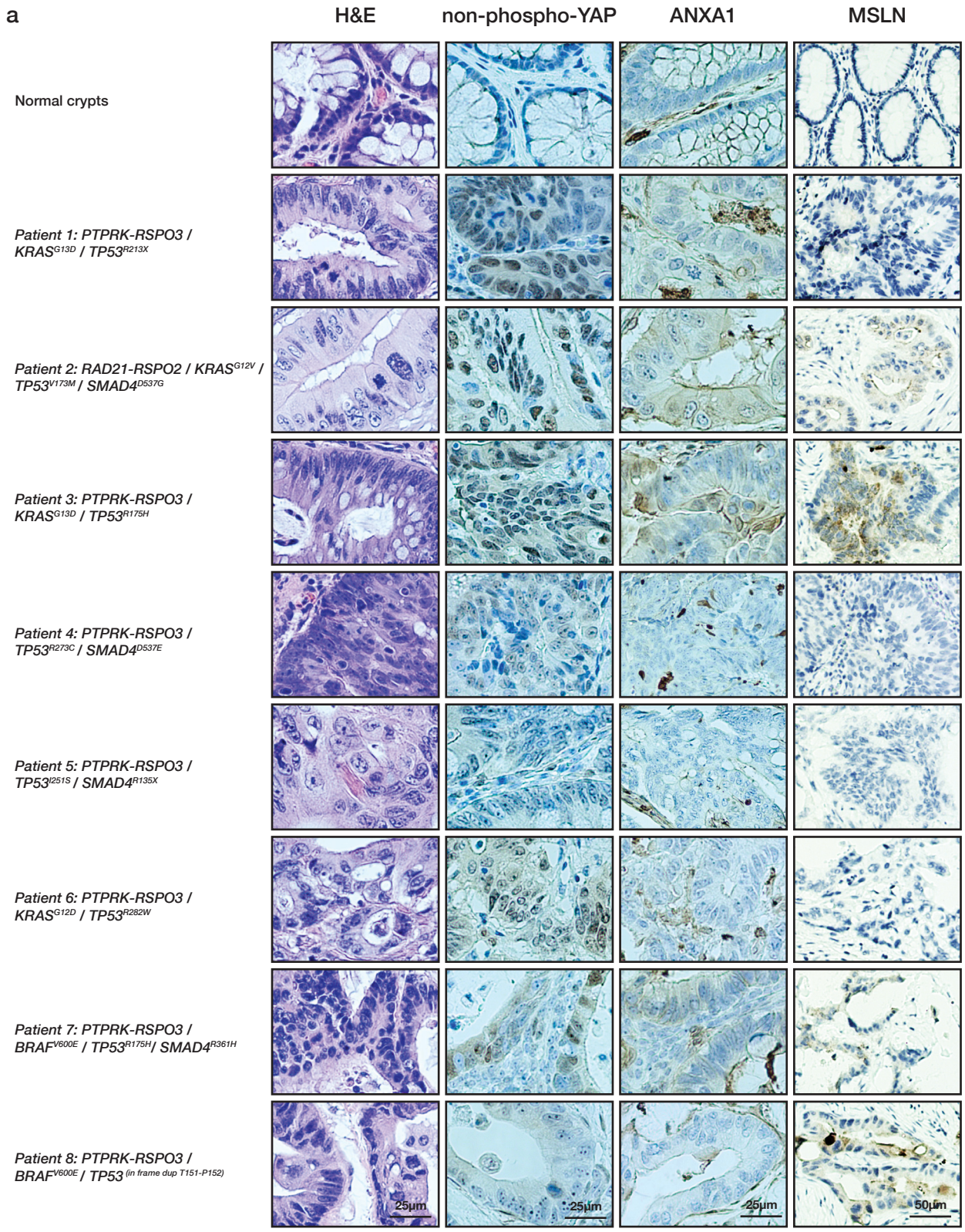

Figure S15. IHC staining of human RSPO2/3 fusion CRCs. **a.** Representative H&E and immunohistochemical stains for active (non-phosphorylated) YAP1, ANXA1, and MSLN in 8 RSPO2 / RSPO3 fusion CRCs. Genotypes of RSPO, KRAS/BRAF, TP53, and SMAD4 are shown on the left. **b.** Classification of staining intensity for each marker across the tumor sections. Pathology assessment was performed blinded to the sample genotype.

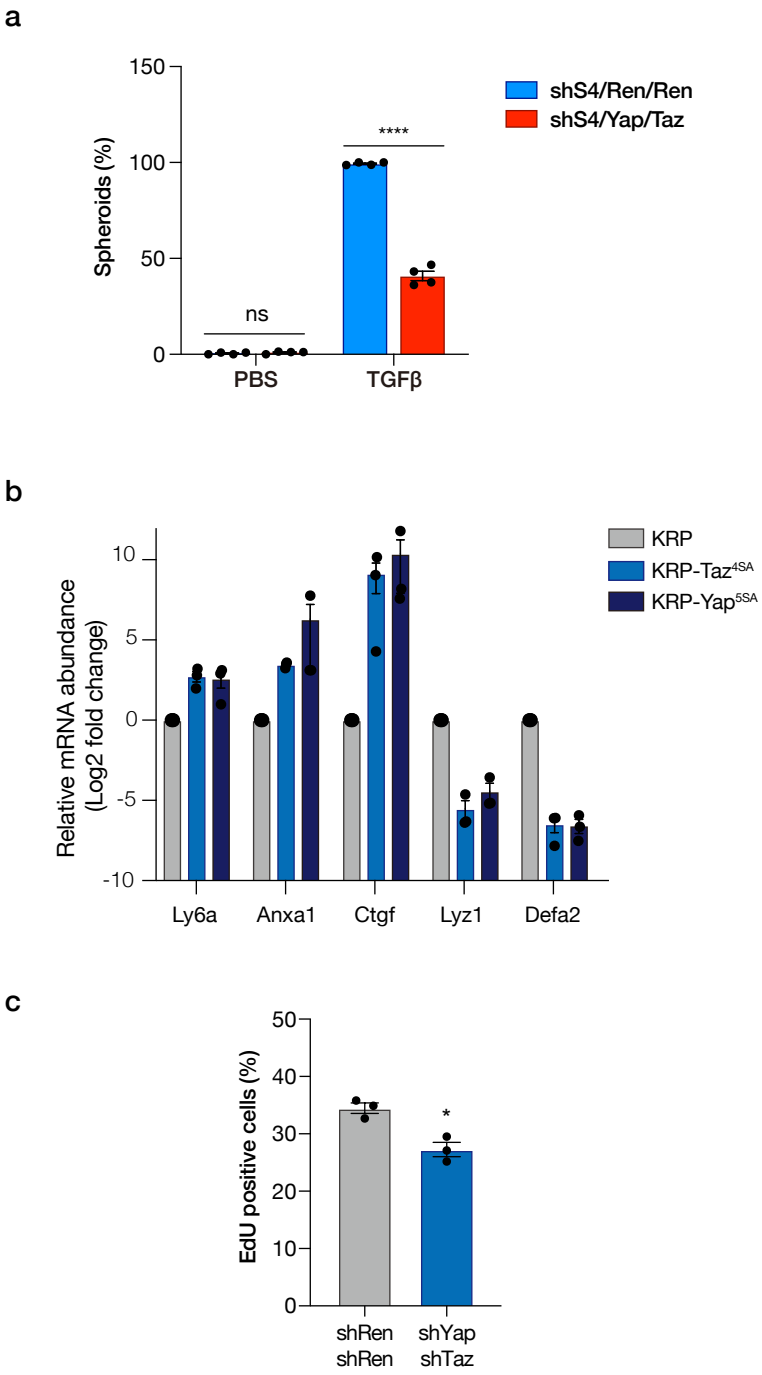

Figure S16. Yap/Taz promotes lineage reversion and WNT independence. a. Quantitation of spheroid formation in TGFβ-treated KRPshS organoids transduced with control (shRen/shRen) or YAP/TAZ (shYap/shTaz) tandem knockdown vectors. Two-way ANOVA, **** $p<0.0001$. **b**. qRT-PCR analysis of gene expression in KRP, KRP-TAZ^{4SA} and KRP-YAP^{5SA} organoids showing induction of YAP/TAZ targets (Ctgf) and fetal markers (Anxa1, Ly6a), and suppression of Paneth cell markers (Lyz1, Defa2). **c.** Percentage EdU positive cells measured by flow cytometry in KRP organoids expressing control (shRen/shRen) or Yap/Taz (shYap/shTaz) tandem shRNA vectors. Error bars are +/- SEM. p-value calculated by two-tailed t-test, n=3, *$p<0.05$.